Available online at www.sciencedirect.com
ScienceDirect
Chemical Physics Letters 449 (2007) 286–290
CHEMICAL PHYSICS LETTERS
www.elsevier.com/locate/cplett

Studies of protonated and anionic artemisinin in the gas-phase by infrared multi-photon dissociation and by negative ion photoelectron spectroscopies

M. Seydou [a], J.C. Gillet [a], X. Li [b], H. Wang [b], G.H. Posner [b], G. Grégoire [a], J.P. Schermann [a], K.H. Bowen [b,*], C. Desfrançois [a]

[a] *Laboratoire de Physique des Lasers, UMR 7538 CNRS, Université Paris 13, Institut Galilée, 93430 Villetaneuse, France*
[b] *Department of Chemistry, Johns Hopkins University, Baltimore, MD 21218, USA*

Received 31 August 2007; in final form 23 October 2007
Available online 30 October 2007

Abstract

Protonated and anionic artemisinin in the gas phase have respectively been studied by infrared multi-photon dissociation (IRMPD) spectroscopy and by anion photoelectron spectroscopy. Comparison of the measured IRMPD spectrum with calculated spectra of various conformations showed that the two lowest-energy protonated structures, both corresponding to protonation at the $C{=}O_{14}$ carbonyl site, were observed experimentally. The calculations also indicated that the peroxide bridge in artemisinin is only slightly modified by protonation. Additionally, stable, intact (parent) artemisinin radical anions have been obtained for the first time in the gas phase and the photoelectron spectrum supports the computational finding that the excess electron is mainly localized on the σ^* orbital of the peroxide bond. The vertical detachment energy and adiabatic electron affinity, calculated at the MP2/6-31+G* level, are in good agreement with the experimental data and the O–O distance is calculated to be stretched by more than 50% in the anion.

The 1,2,4-trioxane artemisinin molecule and some of its derivatives have potent antimalarial activity [1]. For example, some artemisinin-derived trioxane dimers cure malaria-infected mice after only a single subcutaneous dose [2]. Some artemisinin derivatives are also selectively and potently growth inhibitory to human cancer cells [3,4]. Commercial production of artemisinin currently relies on low-yield extraction and purification from Artemisia annua (qinghao) plants. An alternative non-plant source of an immediate precursor to artemisinin has recently been developed via genetic engineering of *Eschericia coli* [5]. The chemical mechanism of antimalarial action of the artemisinin family of trioxanes is generally accepted to involve a ferrous iron-induced one electron reductive cleavage of the trioxane peroxide bond, forming an oxy-anion oxy-radical and subsequently forming several cytotoxic intermediates [1,6].

Several theoretical studies have previously addressed the problem of the structure and reactivity of artemisinin [7–10]. Those quantum chemistry studies, generally conducted at the DFT level, implicitly assume that the considered molecules are isolated from environmental influences. Thus, their predictions are best tested by means of comparison with gas-phase experiments. Recently, electron scattering experiments have also considered the dissociative electron attachment properties of gas-phase artemisinin [11,12]. Here, we provide experimental data concerning the infrared spectrum of protonated artemisinin as well as the photoelectron spectrum of the artemisinin radical anion. These data may be useful as experimental benchmarks for future *in silico* investigations.

As shown in Fig. 1, in which we adopt the atomic numbering of Ref. [7], the artemisinin molecule possesses five

* Corresponding author. Fax: +1410 516 8420.
E-mail addresses: scherman@galilee.univ-paris13.fr (J.P. Schermann), kbowen@jhu.edu (K.H. Bowen), desfranc@galilee.univ-paris13.fr (C. Desfrançois).

0009-2614/$ - see front matter © 2007 Published by Elsevier B.V.
doi:10.1016/j.cplett.2007.10.086

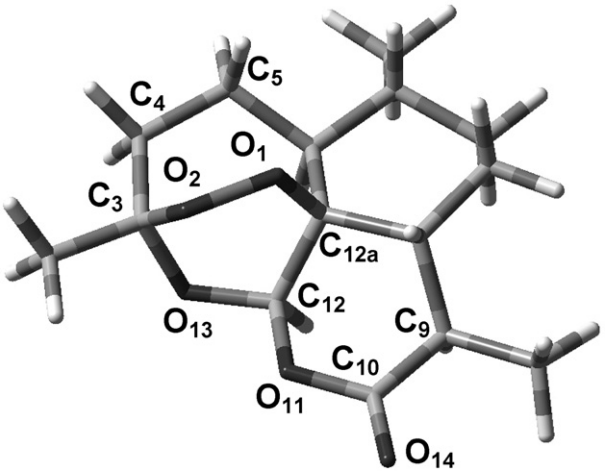

Fig. 1. Atomic numbering for the artemisinin molecule.

oxygen atoms (O_1 and O_2 in the peroxide bridge, O_{11} and O_{13} in the ether rings, and O_{14} in the carbonyl bond) that can potentially act as proton acceptors. The infrared spectrum of protonated artemisinin was measured by infrared multi-photon dissociation (IRMPD) spectroscopy [13] at the free electron laser (FEL) CLIO facility in Orsay (France). The experimental method has been previously described in detail [14]. In brief, protonated artemisinin ions are produced by means of electrospray and are mass-selected in a quadrupole RF trap in the presence of a helium buffer gas at 300 K. Those ions were illuminated during tens of milliseconds by the FEL laser. The IRMPD spectrum, recorded by monitoring the ionic fragmentation yield as a function of the FEL frequency in the 1000–1800 cm^{-1} range, is displayed in Fig. 2. While the positions of the recorded IRMPD spectral lines reflect the infrared absorption spectrum with some weak broadenings and red-shifts [13], their intensities may not, due to differences between internal vibrational redistribution (IVR) rates of the excited vibrational lines [14,15]. The interpretation of this spectrum was conducted by comparing the theoretically-predicted vibrational spectra of different conformers with the experimentally determined spectrum. The minimum structures, the electronic and free energies, and the infrared spectra corresponding to different protonation sites and conformations were calculated at the B3LYP/6-31G* level of theory. All calculated harmonic frequencies were scaled by the same usual factor of 0.9614.

Table 1 displays the calculated relative electronic and free energies, for the six lowest-energy isomers found for the five oxygen protonation sites. As clearly demonstrated by these values, the most favored protonation site is the carbonyl oxygen O_{14}, and we found that two conformers exist, labeled $O_{14}A$ and $O_{14}B$, which differ only by the orientation of the O_{14}–H^+ group: the torsional $C_9C_{10}O_{14}H^+$ angles are about 180° for $O_{14}A$ (H^+ towards O_{11}) and close to 0° for $O_{14}B$ (H^+ towards C_9 methyl group). The equilibrium structures and the simulated spectra are displayed in Fig. 2 for these two conformers. It is seen that the lowest

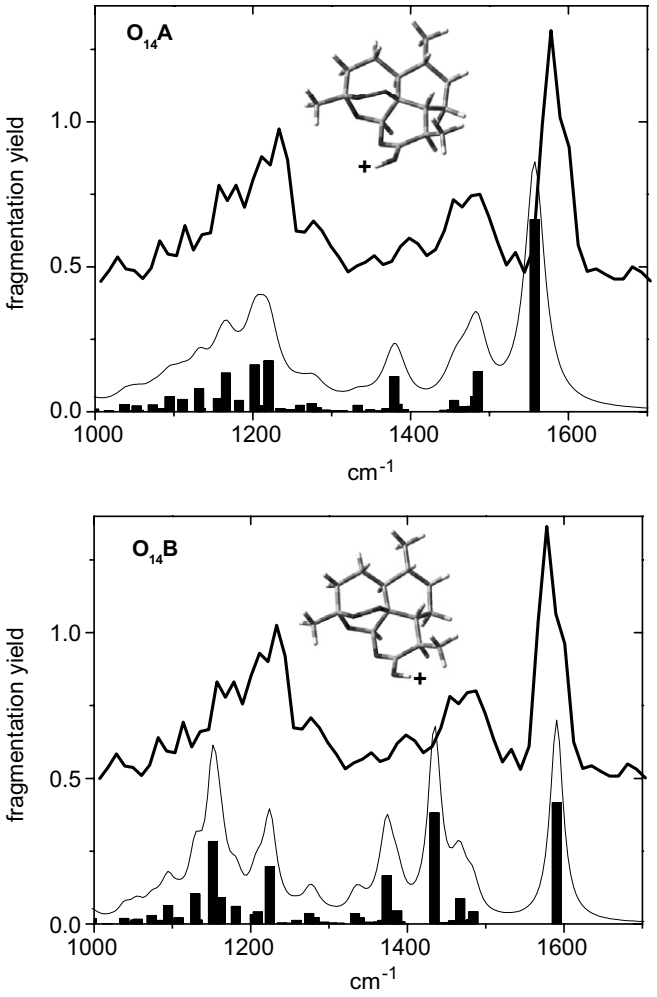

Fig. 2. Experimental (dark trace) and calculated (light trace and sticks) IRMPD spectra of protonated artemisinin for its $O_{14}A$ (top) and its $O_{14}B$ (bottom) conformers. $O_{14}A$ is the lowest-energy minimum, and its simulated spectrum fits well the experimental one. $O_{14}B$ conformer lies 3.9 kcal/mol above $O_{14}A$ and its simulated spectrum fits less well.

Table 1
Relative electronic energies, ΔE, relative free energies, ΔG, and bond length $d_{O_1-O_2}$ between the two peroxide oxygen atoms, as calculated at the B3LYP/6-31G* level for the different protonation sites and structures of gas-phase protonated artemisinin

	Protonation site					
	$O_{14}A$	$O_{14}B$	O_{11}	O_{13}	O_2	O_1
ΔE (eV)	0	0.163	0.816	0.542	0.573	1.288
ΔG (eV)	0	0.169	0.775	0.490	0.532	1.303
$d_{O_1-O_2}$ (Å)	1.481	1.481	1.466	1.490	1.457	1.483

In the neutral species, $d_{O_1-O_2}$ is equal to 1.472Å.

minimum $O_{14}A$ is doing quite well in reproducing the experimental spectrum, especially well in the region 1000–1300 cm^{-1}, still well in the 1300–1500 cm^{-1} range, and with a main peak centered at 1560 cm^{-1}, i.e., on the red side but close to the experimental value of 1580 cm^{-1}. This large peak corresponds to the C_{10}–O_{11} stretch coupled to the C_{10}–O_{14}–H^+ bend mode and is thus characteristic of pro-

tonation on the carbonyl oxygen. For $O_{14}B$, this peak shifts to 1590 cm^{-1}, i.e. on the blue side of the experimental line. In the lower frequency region, the simulated spectrum is less in agreement with the measured spectrum. The IRMPD spectra alone are not sufficient to provide a definitive conclusion. In view of the rather high energy difference between $O_{14}A$ and $O_{14}B$, 0.16–0.17 eV (about 4 kcal/mol), as compared to kT at room temperature, 0.025 eV (about 0.6 kcal/mol), it is likely that the $O_{14}B$ conformer is hardly present in the ion population. We are thus lead to interpret the IRMPD experimental spectrum as consistent with the hypothesis that it is mainly dominated by conformer $O_{14}A$.

As also seen in Table 1, other protonation sites correspond to rather high electronic and free energies that are calculated to be at least about 0.5 eV (about 11 kcal/mol) above the lowest minimum $O_{14}A$. Also, their simulated IR spectra do not fit the experimental spectrum, as it is shown in Fig. 3 for the ether, O_{13}, and the peroxidic, O_2, protonation sites. Thus, protonation sites other than that on the carbonyl oxygen, and in particular those on the peroxide bridge oxygen atoms, correspond to high-energy isomers that are not likely to intervene in protonated biochemical reactions involving artemisinin. Finally, the peroxide internuclear distance $d_{O_1-O_2}$ is only slightly affected by protonation (by less than 0.01–0.02 Å) on any of the five oxygen atoms, even when the proton sits on one of these peroxide oxygen atoms.

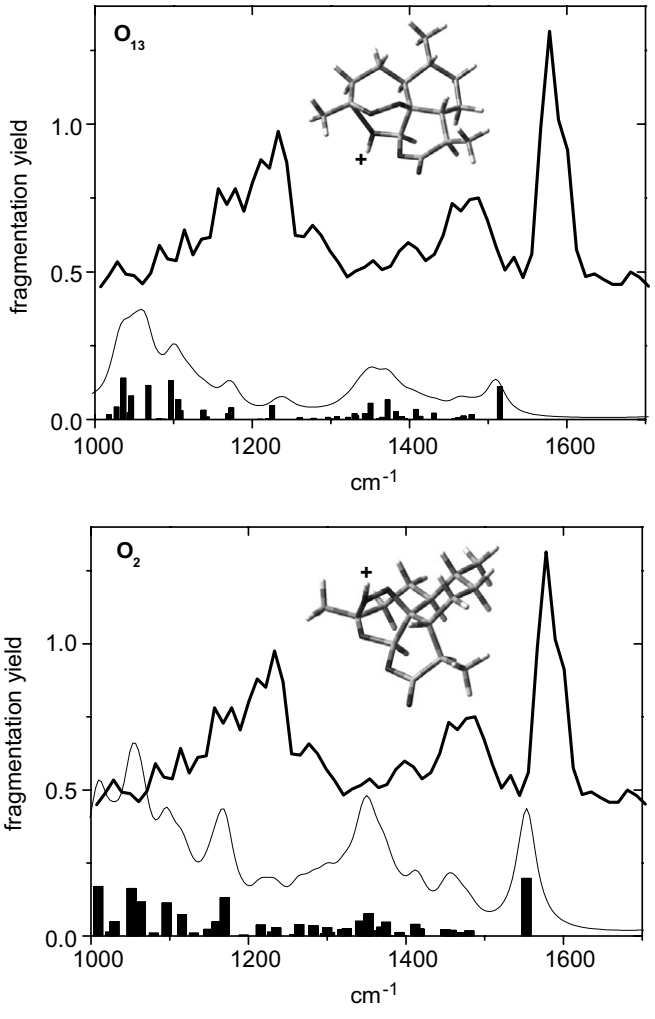

Fig. 3. Experimental (dark trace) and calculated (light trace and sticks) IRMPD spectra of artemisinin protonated at its ether O_{13} (top) or peroxidic O_2 (bottom) oxygen atoms. Neither simulated spectra fit the experimental spectrum. Both simulated spectra correspond to conformers that are calculated to lie at energies which are too high to be present in the ion population at room temperature.

The negative ion mass spectrum of artemisinin, displayed in Fig. 4, has been recorded using a novel anion source in which involatile biomolecules are brought into the gas phase as parent anions [16]. In this source, neutral biomolecules are desorbed with low-power infrared laser pulses, while, almost simultaneously, visible laser pulses generate electrons from a photoemitter, and a pulsed gas valve provides jets of helium. The mass spectrum obtained with this source is dominated by an intense peak corresponding to the loss of CO from artemisinin and a lower intensity peak corresponding to the parent (intact) artemisinin radical anion. This is the first observation of the stable intact anion of artemisinin in the gas phase. Given the strongly anti-bonding σ^* character of the singly occupied orbital of the anion's O_1–O_2 bond, and in view of previous electron transmission and dissociative electron attachment spectroscopic studies [11,12], it was not clear *a priori* that artemisinin would form a stable anion. Since the flight time through the mass spectrometer is $\sim 10^{-5}$ s, the parent artemisinin anions that we observe are living at least that long.

The photoelectron spectrum of the artemisinin anion is presented in Fig. 5. It was recorded by crossing a mass-selected beam of artemisinin parent anions with a fixed-frequency photon beam. The resultant photodetached electrons were energy-analyzed using a magnetic bottle energy

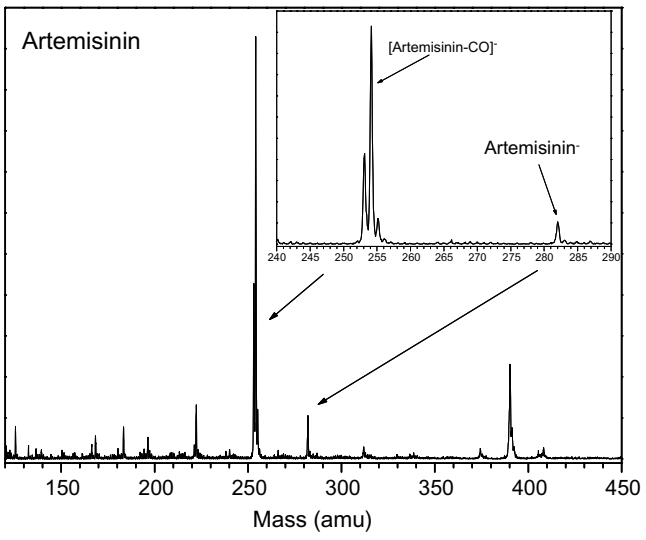

Fig. 4. Negative ion mass spectrum of artemisinin obtained with our laser-desorption/photoemission anion source. The parent negative ion of artemisinin is located at mass 282 a.m.u.

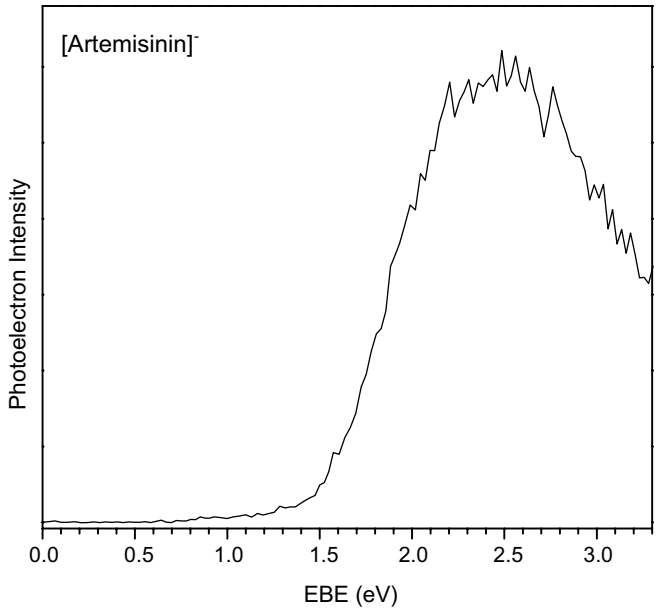

Fig. 5. The photoelectron spectrum of the parent artemisinin radical anion recorded with 3.493 eV photons. The peak maximum, 2.5 eV, corresponds to the vertical detachment energy, while the onset at about 1.4 eV is an estimate of the adiabatic electron affinity.

analyzer with a resolution of 35 meV at EKE = 1 eV. Photodetachment of electrons is governed by the energy-conserving relationship, $h\nu = \mathrm{EBE} + \mathrm{EKE}$, where EBE is the electron binding (transition) energy, EKE is the measured electron kinetic energy, and hν is the photon energy. The vertical detachment energy (VDE) is the energy difference between the anion and its neutral counterpart at the equilibrium geometry of the anion. The adiabatic electron affinity (EA_a) is the energy difference between the ground vibronic state of the neutral and that of its corresponding anion (see Fig. 3 in Ref. [17]). The photoelectron spectrum of the artemisinin anion displays an onset at ~1.4 eV and a peak maximum at 2.5 eV. The former is an approximate upper limit of the EA_a value (assuming minimal hot bands), while the latter is a measurement of the VDE value of the artemisinin anion.

In previous studies on non-dissociative electron capture by disulfide molecules [17], we had shown that an excess electron can be accommodated in the σ^* orbital of a disulfide bond, leading to a stable intact negative ion with a low but positive EA_a value (about 0.1 eV) but with a rather large VDE (about 1.8–1.9 eV) due to the strong stretching of the anion interatomic S–S distance. It was also shown that calculations at the MP2/6-31+G* level were able to give EA and VDE values which slightly underestimated the experimental values (by about 0.1–0.2 eV), while B3LYP calculations overestimated both quantities (by up to 0.5 eV). The present values for artemisinin and its anion were calculated at the MP2/6-31+G* level for equilibrium structures optimized at the B3LYP/6-31+G*, using the GAUSSIAN 03 set of programs [18]. Our calculated VDE value is 2.34 eV, which is in good agreement with the measured value of 2.5 eV, while our calculated EA_a value is 1.17 eV (1.03 eV from the electronic energies and 0.14 eV more from the ZPE difference), which is compatible with the ~1.4 eV onset of photoelectron yield in Fig. 5. (Modelli had previously calculated the EA_a value of artemisinin to be 1.438 eV. [12]). As for disulfides, B3LYP energy calculations appear to be inappropriate for these three electron bonds, since they strongly overestimate the anion stability and lead to VDE = 4.22 eV and $EA_a = 2.15$ eV. Our calculations confirm that the artemisinin anion's excess electron is mainly localized in a σ^* orbital. Upon electron attachment, the peroxide O_1–O_2 bond indeed stretches from 1.47 to 2.26 Å, i.e., a more than 50% lengthening that is even more important than for disulfides (35%). These results are consistent with Modelli's study [12] and with the accepted mechanism by which the peroxide bond undergoes a one electron reduction [19,20].

In conclusion, our IRMPD experiments are consistent with protonation occuring on the carbonyl O_{14} atom. Protonation only slightly affects the peroxide bridge. From our anion calculations, which are consistent with our photoelectron experiments, we have demonstrated that electron attachment to artemisinin goes preferentially to the peroxide bond and can lead to a stable negative ion, in which the O–O distance is stretched by more than 50%.

Acknowledgments

The authors wish to thank Dr. M. Sauvain for suggesting this study and Dr. J. Lemaire and Dr. J.M. Ortéga, of the CLIO Team in Orsay, for their technical assistance. Part of the material in this work (that from KHB's lab) was supported by (US) National Science Foundation under Grant No. CHE-0517337. G.H.P. thanks the (US) National Institutes of Health (Grant AI 34885) for financial support.

References

[1] P.M. O'Neill, G.H. Posner, J. Med. Chem. 47 (2004) 2945.
[2] G.H. Posner, I.H. Paik, W. Chang, K. Borstnik, S. Sinihtaj, A.S. Rosenthal, T.A. Shapiro, J. Med. Chem. 50 (2007) 2515.
[3] G.H. Posner et al., J. Med. Chem. 47 (2004) 1299.
[4] H. Lai, T. Sasaki, N.P. Singh, Expert Opin. Ther. Pat. 9 (2005) 995.
[5] V.J.J. Martin, D.J. Pitera, S.T. Withers, J.D. Newman, J.D. Keasling, Nat. Biotechnol. 21 (2003) 796.
[6] G.H. Posner, Acc. Chem. Res. 37 (2004) 397.
[7] S. Tonmunpheana, S. Irleb, S. Kokpola, V. Parasuka, P. Wolschannb, J. Mol. Struct. (Theochem) 454 (1998) 87.
[8] J.C. Gu, K. Jiang, H. Ji, J. Mol. Struct. (Theochem) 459 (1999) 103.
[9] M.G.B. Drew, J. Metcalfe, F.M.D. Ismail, J. Mol. Struct. (Theochem) 711 (2004) 95.
[10] S.P. Tonmunphean, V. Kokpol, J. Mol. Struct. (Theochem) 724 (2005) 99.
[11] V. Galasso, B. Kovac, A. Modelli, Chem. Phys. 325 (2007) 141.
[12] A. Modelli, V. Galasso, J. Phys. Chem. A 111 (2007) 7787.

[13] J. Oomens, B.G. Sartakov, G. Meijer, G. von Helden, Int. J. Mass Spectrum. 254 (2006) 1–19.
[14] G. Gregoire, M.P. Gaigeot, D.C. Marinica, J. Lemaire, J.P. Schermann, C. Desfrançois, Phys. Chem. Chem. Phys. 9 (2007) 3082.
[15] N.C. Polfer, J. Oomens, S. Suhai, B. Paizs, JACS 127 (2005) 17154.
[16] S.T. Stokes, X. Li, A. Grubisic, J. Ko, K.H. Bowen, J. Chem. Phys. 127 (2007) 084321.
[17] S. Carles et al., J. Phys. Chem. A 105 (2001) 5622.
[18] M. Frisch et al., GAUSSIAN package in I. Gaussian (Ed.), Pittsburg, PA, 2003.
[19] R.L. Donkers, M.S. Workentin, J. Phys. Chem. B 102 (1998) 4061.
[20] F. Najjar, M. Baltas, L. Gorrichon, Y. Moreno, T. Tzedakis, H. Vial, C. Andre-Barres, Eur. J. Org. Chem. 2002 (2002) 3335.